# Simulation Model for Road Cycling Time Trials with a Non-constant Drag Area

Eivind Rømcke[1], Elias Brattli Sørensen[1], Petter Fossan Aas[1], Lars Morten Bardal[1], Steinar Liebe Harneshaug[1], Magnus Lysholm Lian[1], Luca Oggiano[1] and Scott Drawer[2]
[1]*Centre for Sports Facilities and Technology, Norwegian University of Science and Technology, Trondheim, Norway*
[2]*Team INEOS, U.K.*

Keywords: Road Cycling, Time Trial, Simulation, Aerodynamics, Reynolds Number, Drag Area, Mathematical Model.

Abstract: In a time trial in road cycling, the choice of equipment has a great impact on the results. The purpose of this paper is to expand an existing model for road cycling to account for changes in drag coefficient with changes in the Reynolds number of the air flow. The model gives a prediction of the performance of a cyclist given a certain equipment setup. The model may be used to test different setups and identify the fastest one for a given race. Simulations with existing models have given a mean absolute error of 3.87% of the total time. Validation of the model in this paper yielded predictions that had a mean absolute error of 3.22%. The model correctly predicts the fastest setup, but further testing and validation is required to show its statistical accuracy. Potential improvements of the model includes improved data sets to increase precision of the inputs, and thereby reduce simplifications and assumptions.

## 1 INTRODUCTION

### 1.1 Background

In road cycling time trials (TT) there are very small margins that separates the best riders. Being at the very top requires a precise race plan, and factors like choice of bike, wheels, suit and other equipment may be decisive for a winning race. The following physical parameters are considered the most influential in a time trial.

- **Pedaling Power.** The power produced by the rider power input to the system that, along with gravity, balances power losses.
- **Aerodynamics.** Air resistance will greatly affect the velocity, and depends on the rider's position on the bike, equipment, size and wind.
- **Rolling Resistance.** Friction by deformation of tires and roughness of the road surface will introduce a power loss.
- **Mechanical Energy.** The mechanical energy of the rider will change with velocity and altitude in the gravitational field.

Mathematical models of road cycling have been developed in previous publications (E di Prampero et al., 1979); (Olds et al., 1993); (Olds et al., 1995); (Martin et al., 1998); (Dahmen et al., 2011). Previous models do not account for changes in drag area with changes in the Reynolds number of the air flow. Instead, drag area, defined as the product of drag coefficient and frontal area ($C_DA$), is usually set as an approximated constant from experiments. The model developed by (Olds et al., 1995) yielded an mean absolute simulation error of 3.87%. This result is used as a reference for what is considered the maximum acceptable error for the model in this paper.

This model is based on the model introduced by (Martin et al., 1998), often referred to as the Martin model. The Martin model is a mathematical model which accounts for the key parameters influencing the power balance of a cyclist. It is applying the law of preservation of energy in a road cycling context. Equation 1 shows the total power affecting the rider.

$$P_{TOT} = (P_{AT} + P_{RR} + P_{WB} + P_{PE} + P_{KE})\frac{1}{E_c} \quad (1)$$

Here the different terms correspond to the following power contributions.

$P_{AT}$: The wind resistance.

$P_{RR}$: The rolling resistance.

$P_{WB}$: Friction in the wheel bearings.

$P_{PE}$: Changes in potential energy.

$P_{KE}$: Changes in kinetic energy.



Rømcke, E., Sørensen, E., Aas, P., Bardal, L., Harneshaug, S., Lian, M., Oggiano, L. and Drawer, S.
Simulation Model for Road Cycling Time Trials with a Non-constant Drag Area.
DOI: 10.5220/0008165800760083
In *Proceedings of the 7th International Conference on Sport Sciences Research and Technology Support (icSPORTS 2019)*, pages 76-83
ISBN: 978-989-758-383-4

$E_c$ is the power loss factor in the drive train of the bike. Equation 2 shows the total power input of a cyclist modeled and expanded from the terms in Equation 1, where each line corresponds to the respective power contribution described above. The drag area, $C_DA$ was originally set as a constant found from experiments in the Martin model.

$$\begin{aligned} P_{TOT} = \Bigg[ & \frac{1}{2}\rho(C_DA + F_W)V_a^2 V_G \\ & + V_G[\cos(\arctan(G_R))]C_{RR}m_T g \\ & + V_G(91 + 8.7V_G)10^{-3} \\ & + V_G m_T g \sin(\arctan(G_R)) \\ & + \frac{1}{2}(m_T + \frac{I}{r^2})\frac{V_{G,1}^2 - V_{G,0}^2}{\Delta t}\Bigg]\frac{1}{E_C} \end{aligned} \tag{2}$$

Here $\rho$ is air density, $C_D$ is the drag coefficient, A is projected frontal area, $V_a$ is relative velocity, $V_G$ is ground velocity, $G_R$ is road gradient, $m_T$ is total system mass, g is gravitational acceleration and r is wheel radius. $V_{G,0}$ and $V_{G,1}$ represent initial and final ground velocity within a time segment $\Delta t$, respectively. The constant coefficients are described in Chapter 2.3.1.

## 1.2 Objectives

The model developed by Martin (Martin et al., 1998) was used to predict power with a satisfying accuracy on flat tracks with constant drag area. Accounting for Reynolds number dependency of the drag area allows for a more ambitious use of the model. Here the interest lies in attempting to predict what equipment setup will allow the rider to be fastest on a set course, given the conditions on the day of the race. As such, the objective of this modified model is to predict time trials with a mean absolute difference of less than 3.87% of the actual time, and to correctly predict the best equipment setup.

# 2 METHODS

## 2.1 Model Description

The Martin model can be modified to account for variation in $C_DA$ with variations in the Reynolds number of the air flow. To do this, the model must use the effective wind velocity parallel to the riding direction given a certain yaw angle, to return the correct drag area for those conditions. For this model, these values were obtained through wind tunnel testing. However, (Dahmen and Saupe, 2011) point to the use of computational fluid dynamics (CFD) as an alternative to this. $V_a$ from Equation 2 is the effective wind velocity found by calculating the length of the vector sum of the ground velocity, $V_G$ and the wind velocity $V_w$. This is shown in Equation 3.

$$V_a = \sqrt{\Big(V_w \cdot \cos(\phi - \theta) - V_G\Big)^2 + \Big(V_w \cdot \sin(\phi - \theta)\Big)^2} \tag{3}$$

Here the ground velocity, $V_G$, is given as a negative value as the air resistance works in the opposite direction of the rider's direction of travel. The difference between $\phi$ and $\theta$ will provide the angle of the riding direction relative to the wind, where $\phi$ is the riding direction and $\theta$ is the wind direction. The axes are defined in such a way that zero degrees is wind blowing eastwards and the angles increase counter-clockwise. The angle between the rider's velocity vector relative to the ground, and the effective wind velocity is known as the *yaw angle*. This angle is necessary to find the correct drag area.

$$\text{yaw} = \arctan\left(\frac{V_w \cdot \sin(\phi - \theta)}{V_w \cdot \cos(\phi - \theta) - V_G}\right) \tag{4}$$

These values are then used in the calculation of the total power from the wind, as in Equation 5.

$$\begin{aligned} P_{AT} = & \frac{1}{2}\rho\Big(C_DA + F_w\Big) \cdot V_G \\ & \cdot \Bigg(\Big(V_w \cdot \cos(\phi - \theta) - V_G\Big)^2 \\ & + \Big(V_w \cdot \sin(\phi - \theta)\Big)^2\Bigg) \\ & \cdot \cos\big(yaw\big) \end{aligned} \tag{5}$$

To calculate the total time of the race, Equation 5 is inserted into to Equation 2, and then discretized by dividing the course into segments. This is shown in Equation 6, which is solved for $V_G$ to find the velocity of the rider for each segment, $j$. By making the segment small enough, all quantities can be considered constant over the segment.

$$\left[\frac{1}{2}\rho\left(C_DA_j+F_w\right)\cdot V_{G,j}\cdot\left(\left(V_{w,j}\cdot\cos(\phi_j-\theta_j)-V_{G,j}\right)^2+\left(V_{w,j}\cdot\sin(\phi_j-\theta_j)\right)^2\right)\cdot\cos\left(yaw_j\right)+V_{G,j}C_{RR}m_Tg\cos(\arctan(G_{R,j}))+V_{G,j}\left(91+8.7\cdot V_{G,j}\right)\cdot10^{-3}+V_{G,j}m_Tg\sin(\arctan(G_{R,j}))+\left(m_T+\frac{I}{r^2}\right)\frac{V_{G,j}^2-V_{G,j-1}^2}{\frac{L_j}{V_{G,j}}+t_{j-1}}\right]\frac{1}{E_C}-P_j=0 \quad (6)$$

Here, $C_DA$ is interpolated from table values, based on the velocity in the previous segment. The elapsed time per segment is then derived by dividing the segment length, $L_j$ by the segment velocity $V_j$. This is done for all segments, $j$, using all equipment setups, $i$. The logic of the simulation is illustrated in Figure 1, where the total race time for each equipment setup and the velocity profile is calculated.

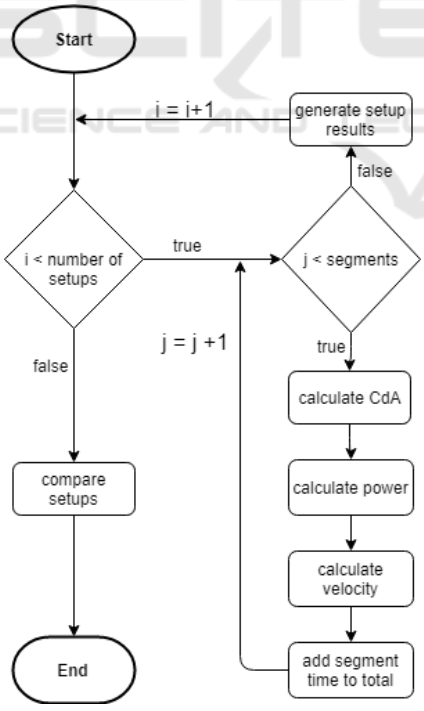


Figure 1: Flowchart showing how the model is used in a discrete context.

The following assumptions are made.

**Weather Conditions.** The wind speed- and direction are assumed to be constant for the whole simulation, making $V_{w,j}$ and $\theta_j$ the same for every segment. In reality, atmospheric wind will always be turbulent over a large range of length scales. Small scale turbulence can alter the flow around the cyclist compared to the low turbulent wind tunnel conditions. Large scale turbulence, also called gustiness, will cause a instant shift in the $C_DA$-velocity-yaw set-point, and also, because of the squared velocity dependency in the drag formula, cause an underestimation of the simulated drag force. Additionally, temperature and air pressure are assumed constant for the whole simulation.

**Turns and Braking.** The model does not account for braking and accelerating in and out of corners. Brake patterns and turning technique varies from corner to corner and rider to rider, thus no general equation was implemented for this.

**Power Input from Rider.** Power input from the rider is intended to be estimated from previous race data as a function of road gradient. It is therefore assumed that the rider will be able to deliver the same power as defined in the power-gradient curve.

## 2.2 Wind Tunnel Measurements

Wind tunnel measurements of two test riders were performed in the wind tunnel at the Norwegian university of science and technology (NTNU) in Trondheim. The wind tunnel has a test section cross-section of 2.7 x 1.8 meters (w x h) and the resulting blockage ratio was $> 10$ %. A blockage correction factor based on CFD simulations was applied to the measured data. A time trial bike was fixed to a 6-component force balance (Carl Schenck AG) supported by aerodynamic struts on the fork and a bike trainer (Tacx Bushido) on the rear hub. The free stream wind speed was measured with a pitot-static tube, and the incoming wind speed was corrected with the cosine of the yaw-angle for the yawed test cases.

A comfortable time-trial position that could be replicated in a field test was chosen by each rider and the drag force along the bike axis was measured with the rider pedaling at a steady cadence. The influence of variation in cadence on aerodynamic drag was investigated and found to be negligible. The drag of the bike support was also measured and subtracted from the total drag. Due to the inherent uncertainty related to rider position and pedaling, 3 measurements of 20 seconds sampling time were made and averaged for each test case. A visual feedback system, including a side view camera and overlaid guide lines, was installed in the wind tunnel in order to aid the test riders maintain the same position for all test cases.

The drag area of the full rider and bike setup was measured at 5 different wind speeds ranging from 30 $km/h$ to 70 $km/h$, and at 4 different yaw angles ranging from 0 to 15 degrees. The resulting data-set covers the conditions most commonly experienced during a flat time-trial. Drag values for simulated cases falling outside of the measured data-set are set to the closest measured value, but these cases are expected to be few under normal race conditions.

## 2.3 Model Validation

### 2.3.1 Determination of Coefficients

The moment of inertia of the wheels, the rotational drag coefficient of the wheels as well as power loss in wheel bearings and chains were taken directly from (Martin et al., 1998). The coefficient of rolling resistance was retrieved from (XBits, 2016) for a tire model similar to the one used on the test bike. The values are listed below.

**Moment of inertia of wheels:** $I = 0.14kg \cdot m^2$

**Rotational drag coefficient:** $F_w = 0.0044$

**Mechanical loss coefficient:** $E_C = 0.976$

**Coefficient of rolling resistance:** $C_{RR} = 0.00297$

### 2.3.2 Field Test

Validation of the model's accuracy was done by conducting tests on a 6.8$km$ course with both flat, uphill and downhill sections. The $C_DA$ data-sets for the two test riders from the wind tunnel was used in the simulations. Wind velocity and -direction, and temperature were measured on site, and the air pressure was retrieved from the weather forecast of the day. Two different test cases were chosen for each of the two test riders, rider 1 testing two different skinsuits and rider 2 testing two different riding positions. The two riders used the same TT-bike and -helmet. Total system mass of the test riders and equipment was measured prior to the test, as listed below.

**Rider 1, Skinsuit 1:** 92.9 $kg$

**Rider 1, Skinsuit 2:** 92.7 $kg$

**Rider 2, Skinsuit 1:** 92.7 $kg$

The course was ridden in both directions; southward with 90$m$ of climbing, and northwards with 19$m$ of climbing. Both with a net elevation gain and loss of 72$m$ respectively. The tests were done with a flying start of 8.5$m/s$ southwards and 12.5$m/s$ northwards. Test rider 1 rode four tests; both directions with two different skinsuits. Test rider 2 did two tests southwards with Skinsuit 1; once seated in an aerodynamic time trial position and one standing up in hills inclined by more than 4%. The bike was equipped with a crank arm based power meter (Stages Cycling LLC), allowing the riders to pace their power output during the test. The riders were instructed to follow the simulated power curve shown in Figure 2.

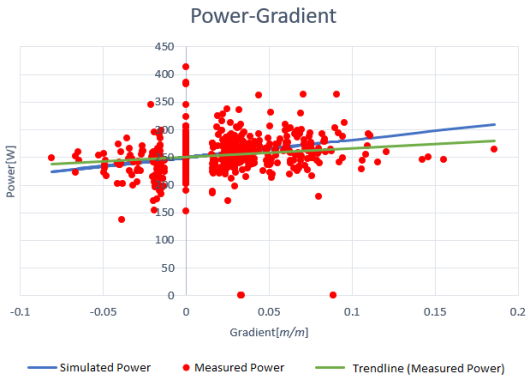


Figure 2: Power curve used in the simulation and measured power for Test rider 1 in Test 1.

The power output for 0% incline was set to 250$W$ with an increase of power per % increase in gradient of 3.2$W$. Elapsed time, velocity and gradient were measured with a Garmin Edge®820 bike computer as well as two independent stopwatches.

The wind conditions varied along the course during the field test. The northernmost 2.43$km$ of the course were exposed to wind while the remaining parts were calm because of the surrounding terrain. Therefore, the course was divided into a northern and southern section, and the test was simulated in two steps; with wind on the northern section, and with zero wind on the rest. The two simulations were then merged. Additionally, the simulations were run with both variable and constant drag area, where the constant drag area was taken from the average velocity of the test and zero yaw.

## 2.4 Subdivisions of Track Segments

A series of simulations of the southbound track was done for Test rider 1 with Skinsuit 1 to find a resolution of segments that yields stable results. Simulations were done with a wind of 0$m/s$, and tested with 2, 5, 10, 20, 40, 80, 160, 320, 640 and 1280 subdivisions of the segments. The default resolution from the GPS-tracker used is 1$s$. Table 1 below shows simulations with the corresponding total simulation time for the different subdivisions.

From the convergence in the graph observed in the table, as well as illustrated in Figure 3, it can be assumed that the result from simulations will not change for simulations with more than 1280 sub-segments. From this, a simulation with 1280 sub-segments can be defined as virtually accurate. An expression can then be made for the relative simulation error with n sub-segments as $e_{v_n,rel} = \frac{v_n - v_{1280}}{v_{1280}}$, where $v_{1280}$ is the es-

Table 1: Simulations of the southbound track for Test rider 1 with Skinsuit 1, wind velocity $0 m/s$.

| Subdivisions | Avg. Velocity | Computation time |
|---|---|---|
| 1 | 8.820 m/s | 0.25 s |
| 2 | 8.783 m/s | 0.5 s |
| 5 | 8.753 m/s | 1.25 s |
| 10 | 8.741 m/s | 2.5 s |
| 20 | 8.735 m/s | 5 s |
| 40 | 8.732 m/s | 10 s |
| 80 | 8.730 m/s | 20 s |
| 160 | 8.729 m/s | 40 s |
| 320 | 8.729 m/s | 80 s |
| 640 | 8.728 m/s | 160 s |
| 1280 | 8.728 m/s | 320 s |

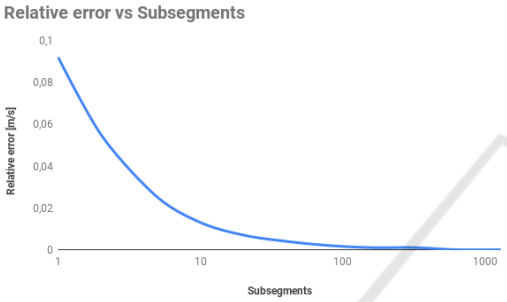


Figure 3: Relative simulation error of average velocity vs. number of sub-segments.

timated average velocity from the simulation with 1280 sub-segments.

Figure 3 shows that the relative error in simulation decreases with an increase in subdivisions, and that the results of the simulations converges monotonically. As shown in Table 1, the simulation time increases with the number of subdivisions. Therefore it is not desirable to choose a very high number of divisions, as the gain in accuracy will be minimal compared to computational cost. The relative error for 40 sub-segments is calculated to 0.05%, with an acceptable total computation time of approximately 10 seconds. Based on this, a segment subdivision of 40, resulting in a segment resolution of $\frac{1}{40} s$, was chosen for the simulations.

# 3 RESULTS

The results of the validation test are summarized in Table 2.

The mean absolute difference of the simulations is 3.22%. In Table 2, the symbols are defined as shown below.

R: Test rider

S: Skinsuit

D: Direction of the test course

Table 2: Results of model validation.

| **Test** | **1** | **2** | **3** | **4** | **5** | **6** |
|---|---|---|---|---|---|---|
| R | 1 | 1 | 1 | 1 | 2 | 2 |
| S | 1 | 1 | 2 | 2 | 1 | 1 |
| D | S | N | S | N | S | S |
| $V_wS$ | 0 | 0 | 0 | 0 | 0 | 0 |
| $V_wN$ | 3.5 | 2 | 2 | 2 | 1 | 1 |
| $dir_w$ | NE | N-NE | N-NW | N-NW | N | N |
| T | 15 | 15 | 15 | 15 | 17 | 17 |
| p | 1018 | 1018 | 1018 | 1018 | 1018 | 1018 |
| P | 254 | 245 | 254 | 244 | 265 | 261 |
| $MAE_P$ | 22.0 | 20.2 | 19.2 | 23.5 | 43.0 | 39.7 |
| $\boldsymbol{t_m}$ | **12:21** | **9:23** | **12:35** | **9:28** | **12:02** | **12:24** |
| $\boldsymbol{t_s}$ | **11:58** | **9:08** | **12:29** | **9:04** | **12:41** | **12:46** |
| $\boldsymbol{e_r}$ | **-3.2%** | **-2.7%** | **-0.82%** | **-4.3%** | **5.4%** | **2.9%** |
| $\boldsymbol{t_{sc}}$ | **11:59** | **09:10** | **12:32** | **9:07** | **12:44** | **12:49** |

$V_wS$: Wind velocity in the southern section $[m/s]$

$V_wN$: Wind velocity in the northern section $[m/s]$

$dir_w$: Wind direction $[orientation]$

T: Temperature [°C]

p: Air pressure [hPa]

P: Average power [W]

$MAE_P$: Mean absolute error of power [W]

$t_m$: Measured time [min : sec]

$t_s$: Simulated time [min : sec]

$e_r$: Relative error between $t_s$ and $t_m$

$t_{sc}$: Simulated time for a constant $C_DA$ [min : sec]

In Test 5 the time-trial position is retained throughout the course, while in test 6 the rider used a standing up position where the gradient exceeded 4%.

Figure 4, 5 and 6 shows the simulated velocity plotted against the measured velocity along the test course, in the southward direction. During the tests, a delay in the gradient measured by the bike computer was observed, meaning that when the gradient changes quickly, such as in transitions into hills or over hilltops, the measured gradient lags behind the terrain. This will result in unrealistic simulated velocities on these sections of the course. Figure 5 also shows a drop in the simulated velocity just before 1000 $m$. This is due to the bike computer measuring a false gradient of 4-5% over a short period at this point. Due to this, the drop in velocity only shows up in the simulation and not in the measured velocity.

# 4 DISCUSSION

As shown in Table 2, the simulated results deviate from the actual time by 0.8%-5.4%. There are primarily two sets of limitations that account for this deviation.

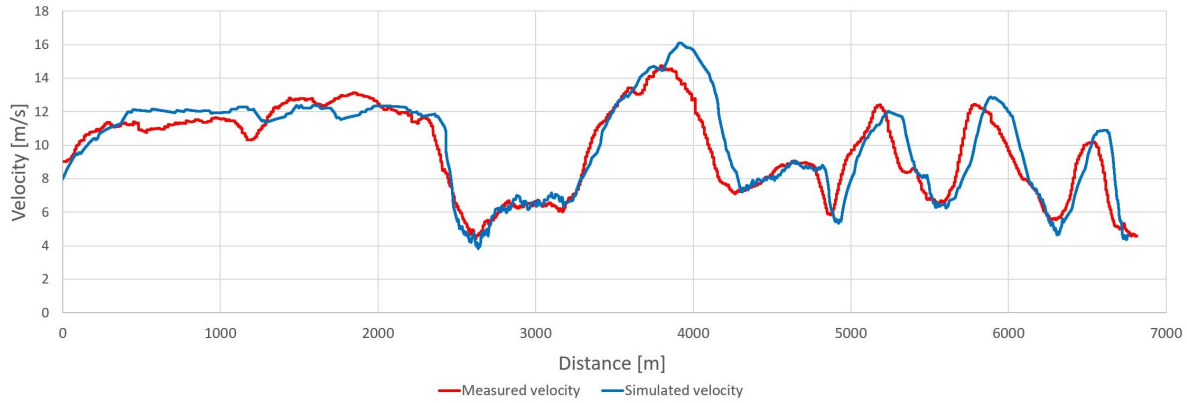


Figure 4: Simulated vs. measured velocity. Test rider 1, Skinsuit 2.

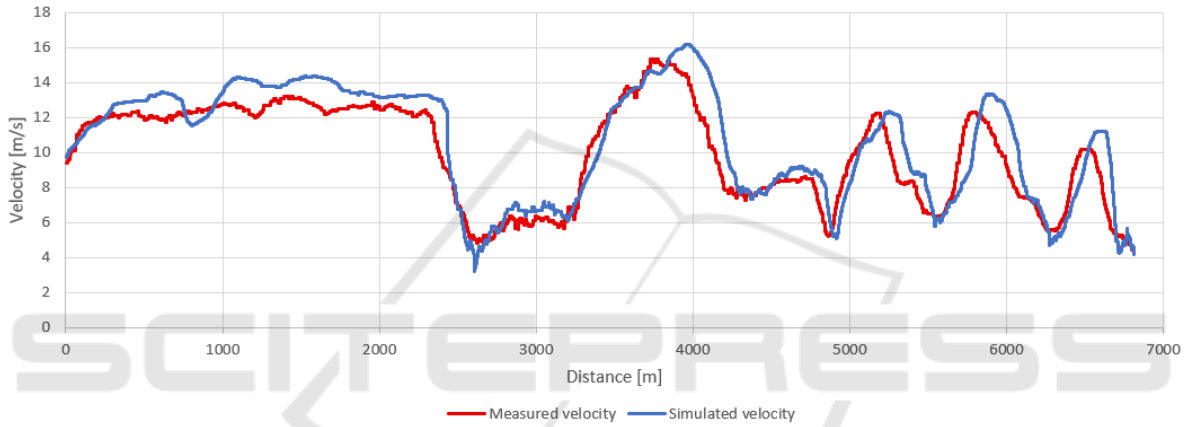


Figure 5: Simulated vs. measured velocity. Test rider 1, Skinsuit 1.

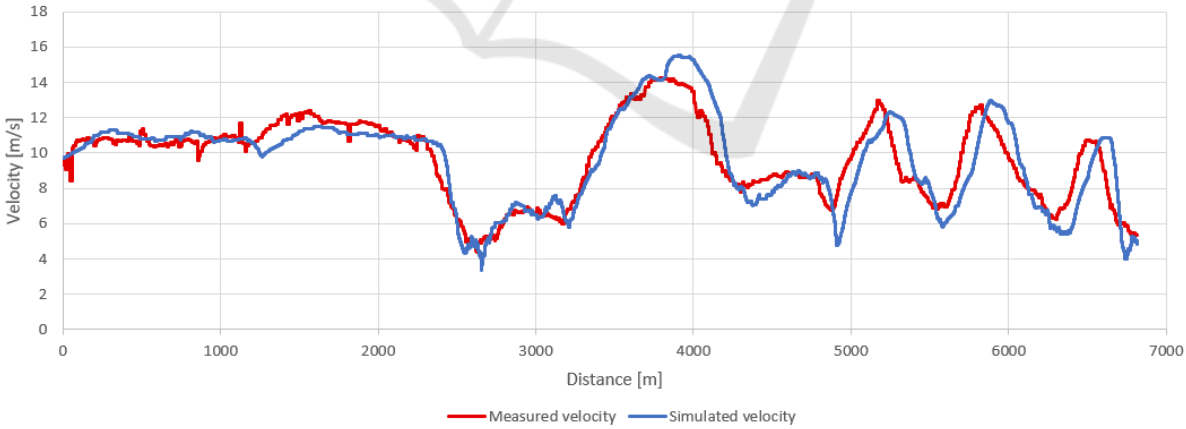


Figure 6: Simulated vs. measured velocity. Test rider 2, Skinsuit 1, standing position on hills.

One is the limitations of assumptions and simplifications that are made for the model. As mentioned in Chapter 2.3.1, values for the coefficients for inertia in the wheels, rotational drag of the wheels, mechanical loss in wheel bearings and chains and rolling resistance were retrieved from previous experiments by other authors. Ideally these coefficients should have been measured for the actual setup used in the test. This uncertainty could have various effects on the results. Furthermore, wind speed and direction are assumed to be constant for a full simulation. This involves a simplification of the actual test conditions, as some of the test runs were susceptible to changes in wind. It was however possible to limit this uncertainty by running

separate simulations, dividing the course into two sections with clear difference in wind conditions. The model does not consider braking and cornering, and this can lead to an underestimation of simulated time for courses with fast downhill sections and sharp turns.

The other set of limitations is the data input to the model. The wind tunnel data were measured for the head down position that a rider normally uses during straight sections of the course, where much attention to the road ahead is not needed. In the validation tests as well as in a race, this will not always be possible, as curves and uneven road surfaces forces the rider to raise their head to scan the road ahead. This will cause the simulated time to be lower than the real time at certain points. However, the time spent in the aero-position increases with the level of the cyclist and is large compared to the time spent in deviating positions for most races. It is shown by (Olds et al., 1995) that riders of a higher level also have a higher discipline of pacing and positioning while riding. As none of the test riders hold international level as cyclists, this effect of this will be greater in the performed tests than for a World Tour rider. Wind tunnel tests were conducted for no lower than $8m/s$ and no greater than $20m/s$. The drag area was assumed constant for any velocities below $8m/s$ and over $20m/s$ in the simulations. The validity of the assumption of a constant drag area is dependant on equipment and position, but the drag area is more likely to increase slightly for lower velocities based on the trend in wind tunnel test results in the Appendix. Velocities below $8m/s$ were measured at some points during climbs and this leads to an underestimation of drag in these hills, thus slightly overestimating the velocity in the simulation. Also a significant uncertainty is related to the instantaneous power produced by the test rider. Even though the average power was fairly consistent between test runs, a random variation around the predefined power curve must be expected. The $MAE_P$ row in Table 2 shows that the mean average error of power input ranged from 19.2 to 43 watts.

Also, the power-slope function developed for this simulation was based on a small data set. Ideally, the power functions should be based on personalized historical performance data for similar race conditions and duration. Another limiting factor of the power curve is that it does not account for a third dimension, namely the length of the race. The average power of a short time trial is significantly higher than that of a long time trial, and the power curve should be scaled accordingly.

It is shown in Figure 4 that the simulated velocity deviates the most from the measured velocity in sections where there is a transition between high and low velocity, typically where the gradient changes quickly, as over a crest and in the transition into a hill. A delay was observed in the gradients recorded by the GPS computer. Due to this delay the simulation will produce unrealistic values in such sections of terrain transition. This results in the simulated velocity curve having close to the same shape as the measured velocity curve, but being shifted slightly to the right. The effect is visible from the $4000m$ mark and onward in Figure 4. More accurate altitude data of the course should lead to more accurate simulations.

Because the wind conditions varied in between the test runs, it is hard to determine with certainty that one equipment setup is indeed faster than the other. The trends observed in the measurements do however indicate that Skinsuit 1 is superior to Skinsuit 2 while riding the course in both directions. When simulating both setups against each other with equal conditions, Skinsuit 1 is predicted to be the faster one of the two. Additionally, the wind tunnel tests results in the Appendix show that Skinsuit 1 gives a lower drag coefficient than Skinsuit 2. This indicates that the model is able to predict which of the setups is the fastest.

In Table 2, results from simulations with a constant drag area are included. Based on the wind tunnel tests results shown in the Appendix, the drag area will vary with velocity (and Reynolds number). The general tendency in these tests was that the predicted time became slightly higher with a constant drag area. It is believed that time trials spanning a greater velocity interval will lead to greater differences between simulations with or without a changing drag area. This will also depend largely on the velocity profile and shape of the $C_D$-velocity curve. For the two skinsuits tested here, the shape of the $C_D$-velocity curves do not intersect and consequently Skinsuit 1 will give a higher velocity throughout the course in both directions.

From the total of six tests that were conducted, the mean absolute error of 3.22% was within the frame of the objectives. Because of the low sample size, in which every test was unique in form of a different rider, equipment setup or course, there is not much basis to name the statistical uncertainty of the simulations. Nor are there enough empirical results to claim that this model of prediction is any more accurate than previous models. However, despite the difficulty of performing accurate field tests involving human test subjects, the test results indicate that the fastest setup identified from the wind tunnel tests, is also faster on the road. Also, given accurate input data, the model should be able to predict the fastest setup for otherwise similar race conditions.

# 5 CONCLUSIONS

Based on the experiments conducted in this paper, the expanded model for predicting road cycling performance may be used to identify the best equipment setup for any given time trial and rider. Simulations of the conducted field tests showed a mean absolute difference of 3.22%, which was within the range of previous

studies. Further experiments and validation is required to determine the statistical uncertainty of the model and the sensitivity to the errors in the various input parameters.

## ACKNOWLEDGEMENTS

We would like to express our gratitude to Team INEOS, and Sondre Bergtun Auganæs of Centre for Sports Facilities and Technology at NTNU for their contributions and support throughout this project.

## REFERENCES

Dahmen, T., Byshko, R., Saupe, D., Röder, M., and Mantler, S. (2011). Validation of a model and a simulator for road cycling on real tracks. *Sports Engineering*, 14(2):95–110.

Dahmen, T. and Saupe, D. (2011). Calibration of a power-speed-model for road cycling using real power and height data. *International Journal of Computer Science in Sport*, 10:18–36.

E di Prampero, P., Cortili, G., Mognoni, P., and Saibene, F. (1979). Equation of motion of a cyclist. *Journal of applied physiology: respiratory, environmental and exercise physiology*, 47:201–6.

Martin, J. C., Milliken, D. L., Cobb, J. E., McFadden, K. L., and Coggan, A. R. (1998). Validation of a mathematical model for road cycling power. *JOURNAL OF APPLIED BIOMECHANICS*, 14(3):276–291.

Olds, T., Norton, K. I., and Craig, N. O. (1993). Mathematical model of cycling performance. *Journal of applied physiology*, 75(2):730–7.

Olds, T. S., Norton, K. I., Lowe, E. L., Olive, S., Reay, F., and Ly, S. (1995). Modeling road-cycling performance. *Journal of Applied Physiology*, 78(4):1596–1611. PMID: 7615475.

XBits, J. B. (2016). Tire test - continental grand prix tt. https://www.bicyclerollingresistance.com/road-bike-reviews/continental-grand-prix-tt-2016. Accessed on 09/04/2019.

## APPENDIX

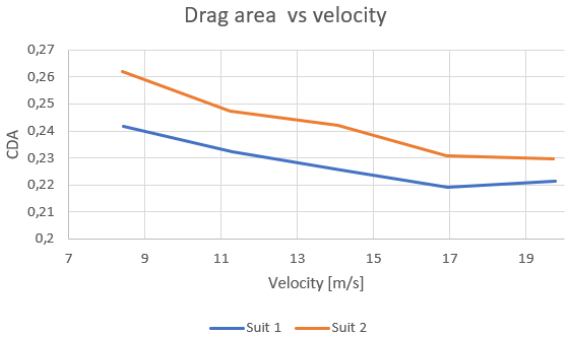


Drag area vs. velocity for Test rider 1 with skinsuit 1 and 2.